J Mater Sci: Mater Electron (2021) 32:28909–28918

A double-functional carbon material as a supercapacitor electrode and hydrogen production: Cu-doped tea factory waste catalyst

S. Özarslan[1], M. R. Atelge[2], Hilal Demir Kıvrak[3], Sabit Horoz[4], Cenk Yavuz[5], M. Kaya[6,*], and S. Ünalan[1]

[1] *Department of Mechanical Engineering, Erciyes University, Kayseri, Turkey*
[2] *Department of Mechanical Engineering, Siirt University, Siirt, Turkey*
[3] *Department of Chemical Engineering, Eskisehir Osmangazi University, Eskisehir, Turkey*
[4] *Department of Electrical-Electronics Engineering, Siirt University, Siirt, Turkey*
[5] *Sakarya University Innovation Center, Sakarya University, Sakarya, Turkey*
[6] *Department of Chemical Engineering, Siirt University, Siirt, Turkey*

Received: 12 July 2021
Accepted: 19 October 2021
Published online: 1 November 2021

ABSTRACT

In the present study, our main aim is to show that the first synthesized metal-doped tea factory waste (TFW) catalyst can be used in both hydrogen production and supercapacitor application. In this context, TFW catalyst doped with copper (Cu) (TFW-Cu) was synthesized for methanolysis of $NaBH_4$ and supercapacitor measurement. In the presence of four different parameters (metal type, metal amount, carbonization temperature, and carbonization time), methanolysis experiments of $NaBH_4$ were performed and the catalyst with the maximum hydrogen production rate (HPR) was determined. As a result, it was determined that the 30% Cu-doped TFW (TFW-30%Cu) catalyst had a maximum HPR at a carbonization temperature of 300 °C and a carbonization time of 60 min compared to other substances. As a result of the methanolysis experiments performed in the presence of TFW-30%Cu catalyst, the maximum HPR and activation energy were determined as 9475 mL $(min.g)^{-1}$ and 13.02 kJ mol^{-1}, respectively. In supercapacitor application, the capacitance of the electrodes in the presence of TFW-30%Cu was calculated as 7–19.9 $F.(g)^{-1}$. Thus, it is expected that the synthesized catalyst will make a promising contribution in both energy storage and energy production areas—especially for distributed generation systems operating in national networks.

Address correspondence to E-mail: mustafakaya@siirt.edu.tr

https://doi.org/10.1007/s10854-021-07275-6

1 Introduction

Energy is needed for production in the world economy. Despite having alternatives, fossil fuels are the most used energy source today. However, fossil fuels pollute the environment, are doomed to run out, and will get more expensive as they decrease [1]. The only way is to offer a healthy and clean world to all humanity; It is the use of renewable energy resources such as solar, wind, and biowaste. However, hydrogen draws attention in that it is in a position to meet the world's enormous energy needs due to its storability. Hydrogen is abundant in nature and is an efficient energy carrier. With these features, it is possible to use it in many areas, especially transportation and storage technologies [2]. However, the most critical point in hydrogen energy production is its efficient and safe storage and supply. Metal hydrides are a promising option for the storage of hydrogen energy. Fast hydrogen absorption and desorption kinetics, easy activation, low cost, and ease of manufacture can be cited as important properties of metal hydrides for hydrogen storage [3, 4]. Sodium borohydride ($NaBH_4$) is the most efficient among hydrides because it is stable, cheap, and not flammable and not harmful to health. It is possible to produce hydrogen at ambient temperature without additional heating, with additives of catalysts that help obtain high-purity H_2 from $NaBH_4$ [5, 6].

Catalysts are chemical compounds that increase the rate of reaction without they react. Materials such as platinum and palladium have been used as catalysts in the literature [7–9]. However, the use of these materials has disadvantages such as complex preparation, high cost, and intense energy consumption [10]. For this reason, it is important to use cheaper and efficient materials. Another way to accelerate the hydrogen synthesis reaction from sodium borohydride is to use various solvents, particularly alcohol, instead of using water. Recently, it is noteworthy that the methanolysis of $NaHB_4$ is suitable for hydrogen production [11, 12]. The methanolysis of $NaBH_4$ is given in Eq. (1):

$$NaBH_4 + 4CH_3OH \rightarrow NaB(OCH_3)_4 + 4H_2. \quad (1)$$

Furthermore, catalysts can be used as electrode ingredients in the generation of supercapacitors with high-capacity energy stores. Supercapacitors are very advantageous over conventional capacitors. These advantages can be shown as being fast charging, high cyclic life, cost effective, and safe. Thinking about distributed generation (DG) systems and their penetration into the electricity networks, there can be natural and unpredictable problems. Thinking about both solar and wind systems sudden peaks, lack of sunlight, excessive wind, or absence of wind can easily be witnessed. In such occasions, supercapacitors can serve as the best back-up plan instead of UPS Systems with their pre-mentioned abilities. However, deficiencies in raw material type and production methods while developing electrode material reduce the electrochemical performance of supercapacitors [13]. Therefore, it has become an interesting subject to develop electrode ingredients with high capacity and cycle performance in this field. Materials such as activated carbon and carbon nanotube are known to have excellent capacitive performance. However, these materials are not useful because they are difficult and costly to synthesize. As an alternative to these, biomass resources are candidates to be ideal materials with their abundant availability, affordable cost, and relatively high carbon content [14–16]. Tea factory waste (TFW) is a source of biomass generated in tea factories en masse in significant amounts each year. The unused dust, stem, and fiber parts of the tea plant create tea factory waste.

In this study, it was reported as the synthesis of metal-doped TFW catalyst and its application of hydrogen production and supercapacitor. In this context, TFW catalyst doped with copper (Cu) (TFW-Cu) was synthesized for methanolysis of $NaBH_4$ and supercapacitor measurement, and the obtained observations were interpreted.

2 Experimental part

2.1 Preparation of tea factory waste-Cu catalyst

Tea factory waste (TFW) obtained from a tea factory belonging to Çaykur located in the Eastern Black Sea Region of Turkey was used as biomass source. TFW, which was released during the production of black tea in the factories, consisted of the unused powder, stem, and fiber parts of the tea leaves. In the preparation stage, Cu (1.2 g)-doped TFW (0.4 g) was treated with acetic acid (40 mL) and dried in a furnace at 80 °C for 24 h. It was then carbonized in the oven at

300 °C for 60 min. The final sample was washed with pure water and dried in the furnace. The methanolysis experiments of $NaBH_4$ were performed in the presence of different catalyst amounts (0.05–0.2 g), $NaBH_4$ ratios (0.1–0.75 g), and temperatures (30–60 °C).

2.2 Preparation of electrodes prepared from TFW-Cu catalyst

The TFW-30%Cu catalyst was blended with nafion for developing the electrode. For the preparation of supercapacitor electrodes, 80% TFW-30%Cu catalyst, 10% activated carbon, and 10% binder (polyvinylidene fluoride and nafion) were used. The materials were made homogeneous by mixing in the mixer for 2 h. Then the mixture was sprayed on nickel foam. The prepared sample was dried in an oven at 80 °C. It was then cut in a circular shape to accommodate the aluminum cell. The cell was wetted using 6 M KOH electrolyte solution. Electrochemical characterization of the supercapacitor cell was carried out utilizing cyclic voltammetry (CV), electrochemical impedance spectroscopy (EIS), and galvanostatic charged discharge (GCD) practices.

3 Results and discussion

3.1 FTIR analysis

Figure 1 shows Fourier transform infrared spectroscopy (FTIR) spectra of TFW-30%Cu and TFW.

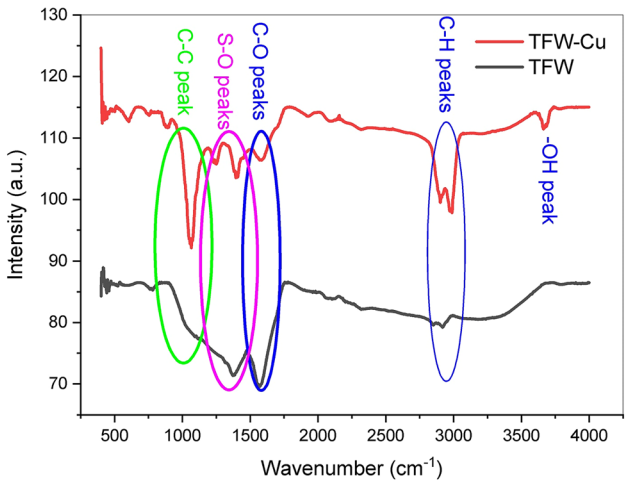

Fig. 1 FTIR spectrum of TFW (black line) and TFW-Cu catalyst (red line) (Color figure online)

FTIR analysis was applied in the wavelength range of 450–4000 $(cm)^{-1}$ in order to comparatively analyze the chemical bonds in the structure of the samples. The peak of hydroxyl group (–OH) was observed at 3676.2 $(cm)^{-1}$ in the FTIR spectrum of TFW-30%Cu catalyst (red line) while hydroxyl group (–OH) was not seen in spectrum of TFW catalyst (black line). Strong peaks represented that the C–H groups were observed in the range of about 2000–3000 $(cm)^{-1}$. The indicator of the presence of the C–O group was observed at 1605.7 $(cm)^{-1}$ in the spectrum of TFW-30%Cu and at 1583.9 $(cm)^{-1}$ in the spectrum of TFW catalyst. The peaks appeared in the range of about 1300 to 1000 $(cm)^{-1}$ could be attributed to the S–O peaks. Moreover, the C–C stretching peak was observed at 1014.2 $(cm)^{-1}$ [17–19].

3.2 SEM–EDX analysis

Figure 2 shows the SEM–EDX images of TFW and TFW-30%Cu catalysts. It was observed that the surface of the TFW was relatively smooth (Fig. 2a) while the surface of TFW-30%Cu was quite rough (Fig. 2c). In the SEM image of TFW-30%Cu catalyst, it observed formation of micro-pores and an increase in the number of particles. It could be said that an observed increase in the roughness and micro-pores could be a reason for an improvement in the catalytic activity of the catalyst.

In the EDX spectrum of the pure TFW catalyst (Fig. 2b), the observed C, O, K, and Mg values were 54.34, 43.88, 1.54, and 0.24%, respectively. In the EDX spectrum of the pure TFW catalyst (Fig. 2b), the observed C, O, K, and Mg values were 54.34, 43.88, 1.54, and 0.24%, respectively. Compared to this spectrum, considering the EDX spectrum of the TFW-30%Cu catalyst shown in Fig. 2d, the C and Cu values were found as 62.53 and 13.30%, respectively. Thus, the increase in C value in the TFW-30%Cu catalyst is worth noting.

3.3 XRD analysis

As can be seen in Fig. 3, X-ray diffractometer (XRD) was utilized for analyzing the structure and phase of pure TFW and TFW-30%Cu catalysts. The scanning range was 2θ = 20°–80°. When the XRD patterns of the two catalysts are compared, it is clearly seen that the amorphous TFW catalyst turns into a polycrystalline structure in the presence of Cu metal. 2

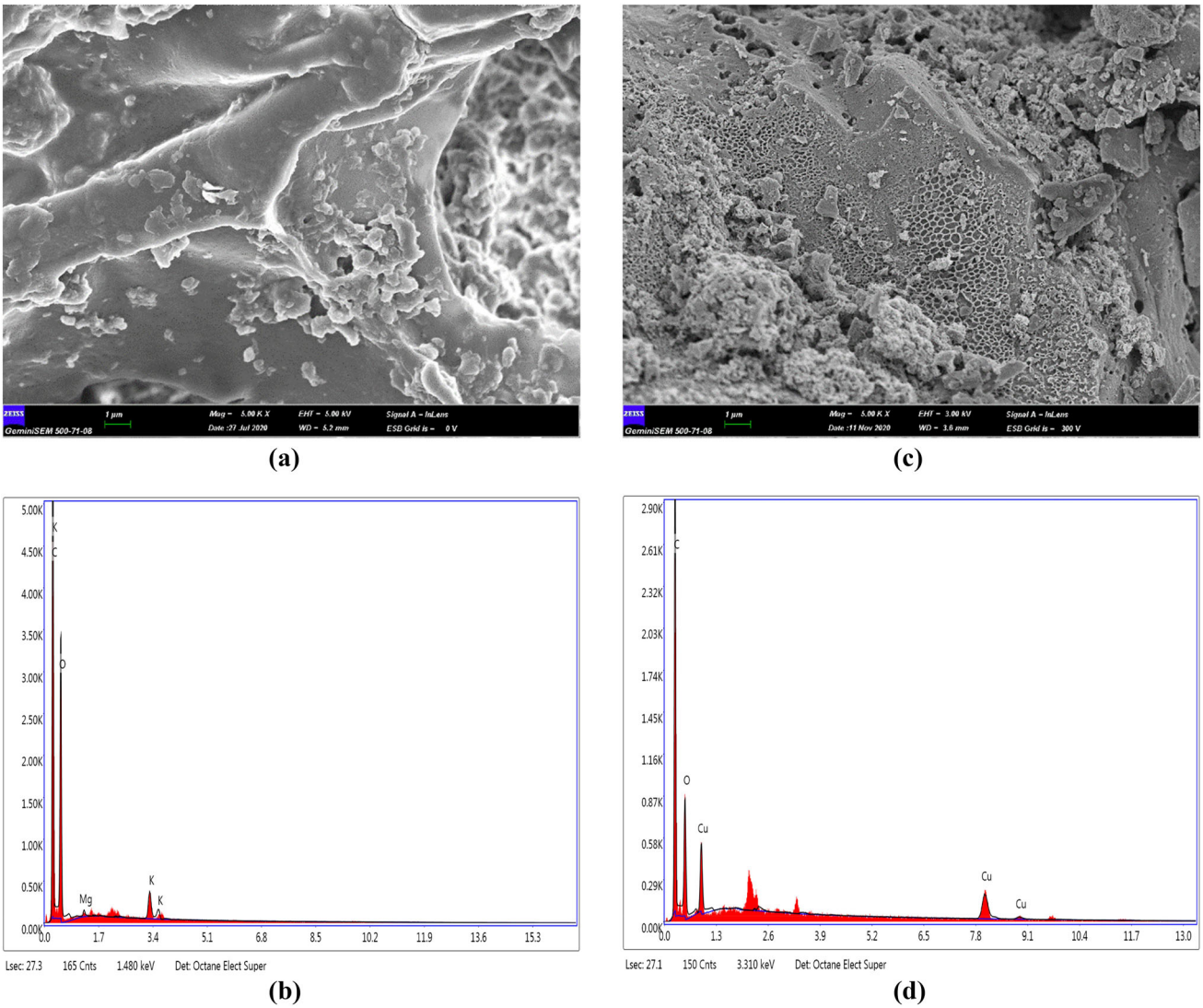

Fig. 2 SEM micrograph of pure TFW (**a**), SEM image of TFW catalyst, (**b**) EDX spectrum of TFW catalyst, (**c**) SEM image of TFW-30%Cu catalyst, and (**d**) EDX spectrum of TFW-30%Cu catalyst

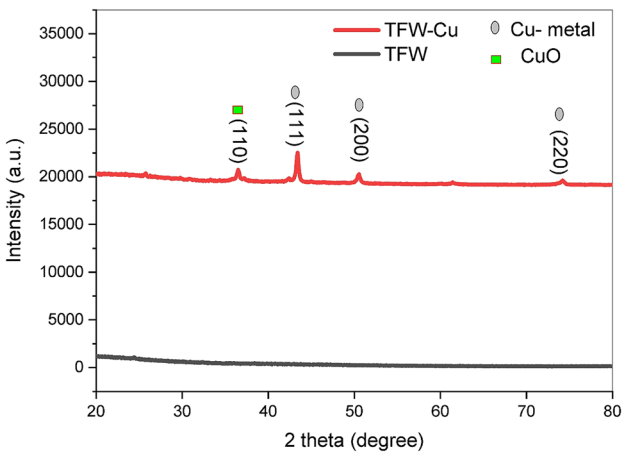

Fig. 3 XRD patterns for TFW and TFW-30%Cu catalyst

theta = 43.50°, 50.63°, and 74.29° correspond to the (111), (200), and (220) planes of Cu metal in hydrotalcite structure [JCPDS 35-0965], respectively. The diffraction pattern corresponding to the (110) plane of CuO at 2 theta = 36.59° is thought to have appeared as a result of carbonization.

3.4 Effect of different substances

In the present study, first, TFW catalyst was doped with different substances such as KNO_3, EDTA, $CoCl_26H_2O$, $MgCl_2$, $CuSO_45H_2O$, and $N_2NiO_66H_2O$ in order to determine what the most effective doped material was, and methanolysis experiments of $NaBH_4$ were carried out in the presence of these

doped catalysts. The parameters were $NaBH_4$ (2.5%), catalyst amount (0.1 g), methanol (10 mL), and temperature (30 °C). The obtained graph of hydrogen volume versus time for different doped catalysts are indicated in Fig. 4. According to Fig. 4 and Fig. 4 (inset), TFW catalyst doped with Cu (TFW-Cu) catalyst has shorter reaction completion time (4 min) and higher HPR value [3687.6 mL $(min.g)^{-1}$] compared to other doped catalysts.

3.5 Effect of Cu-metal concentration

In order to determine the optimum Cu-metal concentration, TFW catalyst was doped with Cu metal at different concentrations (10, 20, 30, 40, and 50%) and methanolysis experiments were carried out in the presence of these catalysts. The parameters were $NaBH_4$ (2.5%), catalyst amount (0.1 g), methanol (10 mL), and temperature (30 °C). The obtained graph of hydrogen volume versus time for different Cu concentrations is shown in Fig. 5. According to Fig. 5 and Fig. 5 (inset), TFW catalyst doped with 30% Cu (TFW-30%Cu) catalyst has shorter reaction completion time (4 min) and higher HPR value [3687.6 mL $(min.g)^{-1}$] compared to other Cu-metal concentrations. Similar observation was reported by Saka et al. They concluded that 30%Cu-B-doped *Chlorella vulgaris* microalgae catalyst had the the shortest completion time and the maximum HPR value [20].

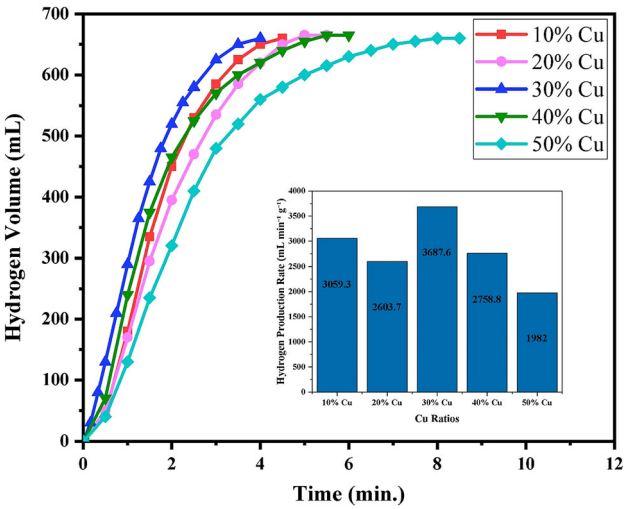

Fig. 5 The graph of hydrogen volume versus time for different Cu concentrations. Inset: The HPR versus different Cu concentrations

3.6 Effect of carbonization temperature

After the optimum Cu-metal concentration was determined as 30%, TFW-30%Cu catalyst was subjected to carbonization process at different temperatures (200, 300, 400, 500 °C) to examine the effect of carbonization temperature, which is another parameter, on the hydrogen production rate and to observe the optimum carbonization temperature. The parameters were $NaBH_4$ (2.5%), catalyst amount (0.1 g), methanol (10 mL), and temperature (30 °C). Figure 6 and the inset of Fig. 6 indicate the graph of

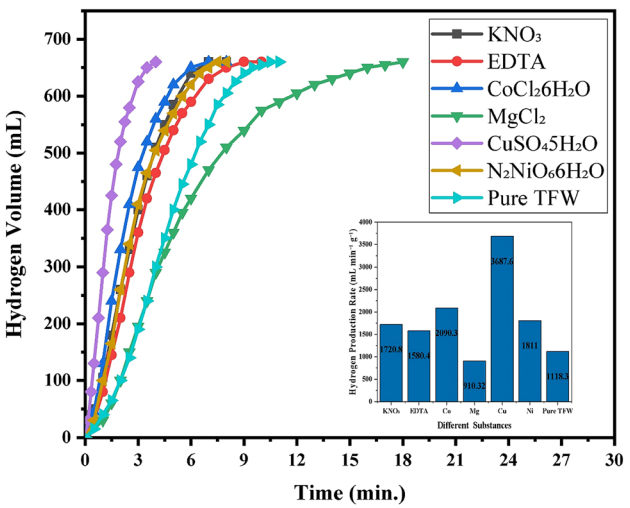

Fig. 4 The graph of hydrogen volume versus time for different doped TFW catalysts. Inset: The HPR versus different doped TFW catalysts

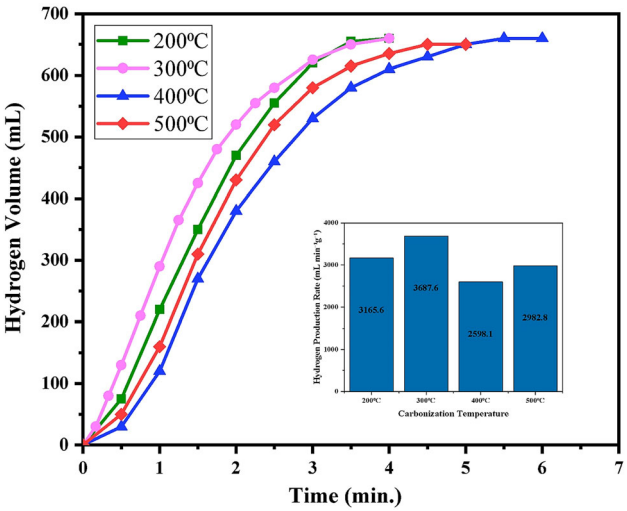

Fig. 6 The graph of hydrogen volume versus time for different carbonization temperatures. Inset: The HPR versus different carbonization temperatures

hydrogen volume versus time for different carbonization temperatures and the graph of HPR versus carbonization temperature, respectively. According to the inset of Fig. 6, the obtained HPR value for 200, 300, 400, and 500 °C is 3165.6, 3687.6, 2598.1, and 2982.8 mL $(min.g)^{-1}$, respectively. Thus, it can be concluded for this study that the optimum carbonization temperature is 300 °C.

3.7 Effect of carbonization time

After the optimum carbonization temperature was determined as 300 °C, studies were conducted to determine the optimum carbonization time. In this context, methanolysis experiments of $NaBH_4$ were carried out at four different carbonization times (30, 45, 60, and 75 min). The parameters were $NaBH_4$ (2.5%), catalyst amount (0.1 g), methanol (10 mL), and temperature (30 °C). Figure 7 and the inset of Fig. 7 show the graph of hydrogen volume versus time for different carbonization times and the graph of HPR versus carbonization time, respectively. When the carbonization times were compared, it was observed that both the methanolysis reaction took a shorter time (4 min) and the maximum HPR value [3687.6 mL $(min.g)^{-1}$] was obtained in the carbonization time of 60 min.

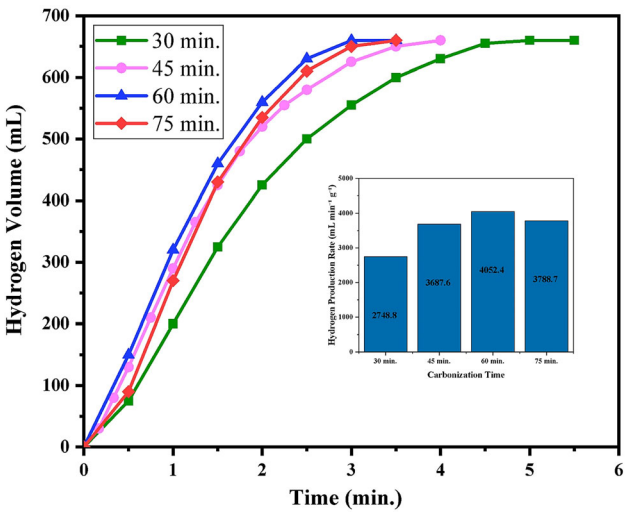

Fig. 7 The graph of hydrogen volume versus time for different carbonization times. Inset: The HPR versus different carbonization times

3.8 Effect of catalyst amount

In order to investigate the effect of catalyst amount on hydrogen production rate, methanolysis experiments of $NaBH_4$ in the presence of different catalyst amount (0.05, 0.1, 0.15, and 0.2 g) were carried out under the same conditions. The graph of hydrogen volume versus time for different catalyst amounts and the graph of HPR versus catalyst amount are indicated in Fig. S1 and inset of Fig. S1, respectively. In order to investigate the effect of catalyst amount on hydrogen production rate, methanolysis experiments of NaBH4 in the presence of different catalyst amount (0.05, 0.1, 0.15, and 0.2 g) were carried out under the same conditions.

As a result of these experiments, two important observations were recorded. First, the maximum HPR value was determined to be 5733 mL $(min.g)^{-1}$ in the presence of 0.05 g catalyst compared to other catalyst amounts. The second important observation is that the increase in the amount of catalyst shortens the methanolysis reaction time. Similar results were reported in experiments performed by Kaya and Bekiroğulları [21] and Fernandes et al. [22]. They concluded that the reaction $NaBH_4$ was catalyst controlled.

3.9 Effect of $NaBH_4$ concentration

In order to investigate the effect of $NaBH_4$ concentration on hydrogen production rate, methanolysis experiments of $NaBH_4$ in the presence of different NaBH4 concentrations (0.10, 0.25, 0.50, and 0.75 g) were carried out under the same conditions. The graph of hydrogen volume versus time for different $NaBH_4$ concentrations and the graph of HPR versus $NaBH_4$ concentration are revealed in Fig. S2 and inset of Fig. S2, respectively. The maximum HPR value was determined as 6072.1 mL $(min.g)^{-1}$ in the presence of 0.75 g $NaBH_4$ compared to other $NaBH_4$ concentrations. Moreover, as a result of the experiments, it was noted that the increase in the concentration of $NaBH_4$ caused the methanolysis reaction of $NaBH_4$ to be completed in a longer time. This is most likely owing to the fact that as the reaction progresses, the concentration of the reaction product $NaBO_2$ [23] ultimately surpasses its solubility limit and precipitates out of solution for this level of $NaBH_4$ concentration. This material may obstruct catalyst sites, slowing down the process [24].

3.10 Effect of temperature

In order to investigate the effect of temperature on hydrogen production rate, methanolysis experiments of $NaBH_4$ at different temperatures (30, 40, 50, and 60 °C) were carried out under the same conditions. The graph of hydrogen volume versus time for different temperatures and the graph of HPR versus temperature are revealed in Fig. S3 and inset of Fig. S3, respectively. It was observed that the increase in temperature both shortened the reaction time and increased the HPR value. As expected [25] that the increase in temperature both shortens the reaction time and increases the HPR value [26]. The maximum HPR value was determined as 9479 mL $(min.g)^{-1}$ at 60 °C.

The activation energy (Ea) is an important parameter for the research about the reaction kinetics. The HPR constant k at different temperature (T) can be determined on the basis of the slope of the fitting line and the ideal gas state equation. The Arrhenius plot of lnk versus 1/T is shown in Fig. S4. The activation energy (Ea) can be calculated by the Arrhenius relation given in Eq. (2) to be 13.02 kJ mol^{-1}.

$$\ln k = \ln a - Ea/RT, \tag{2}$$

where k refers to reaction rate constant, a refers to reaction constant, Ea refers activation energy kJ mol^{-1}, T refers to experiment temperature in Kelvin, and R refers to ideal gas constant.

For comparison purposes, HPR and Ea values obtained in the presence of some metals are given in Table 1.

Hence, the result indicates that the as-obtained TFW-30%Cu catalyst in the present work shows high catalytic activity for hydrogen production from methanolysis experiments of $NaBH_4$.

3.11 Electrochemical characterization of TFW-30%Cu catalyst as electrode ingredient prepared using nafion for supercapacitor cell

In Fig. 8, CV measurement was performed with a potentiodynamic electrochemical technique at different speeds to determine the time-corresponding electrode potential of the TFW-30%Cu catalyst. It was observed that the peaks shifted while the current density increased at high scanning speeds. The large areas obtained in the CV curves can be attributed to the strong supercapacitive response. The impedance spectra of the TFW-30%Cu catalyst given as the Nyquist plot are shown in Fig. 9. The semicircle seen in the Fig. 9 at medium frequency indicates the presence of interface resistance. An excellent resistance was obtained by determining the equivalent series resistance of the electrode at high frequency as 0.62 Ω. The angle of the curve was determined as 78°, indicating that it has good diffusion resistance[31, 32].

Figure 10 shows that the GCD curves belong to electrode exhibit relatively triangular shapes and symmetry at 0.5, 1 and 2 $A.(g)^{-1}$ current intensities. This indicates an effective ion diffusion and a low transport resistance [33, 34]. Using the galvanostatic charge–discharge graphs, the capacitance of the electrodes can be determined by Eq. (3):

$$C = \frac{2I\Delta t}{m\Delta V}, \tag{3}$$

where I (A) is the current, Δt (s) is the discharge time, ΔV (V) is the potential difference, and m (g) is the active mass of an electrode. The electrode capacitance was calculated as 7 $F.(g)^{-1}$ for 2 $A.(g)^{-1}$, 13 $F.(g)^{-1}$ for 1 $A.(g)^{-1}$, and 19.875 $F.(g)^{-1}$ for 0.5 $A.(g)^{-1}$. It is seen that the supercapacitor electrode produced using

Table 1 HPR and Ea values obtained from different studies

Catalyst prepared from biowaste	HPR [mL $(min.g)^{-1}$]	Ea (kJ mol^{-1})	References
Co-B-*Chlorella vulgaris*	13,215	25.22	[27]
SSMS-CH_3COOH-NiB (30wt%) (microalgae strain-based catalyst)	3407	28.8	[23]
Co-Mo-B	1280	51	[28]
DSCG-Zn	8510	7.87	[29]
Metallurgic sludge	9366	48.05	[30]
SSMS-$ZnCl_2$-CoB (methanolysis)	9266	31.13	[12]
TFW-30%Cu (60 °C)	9479	13.02	This study

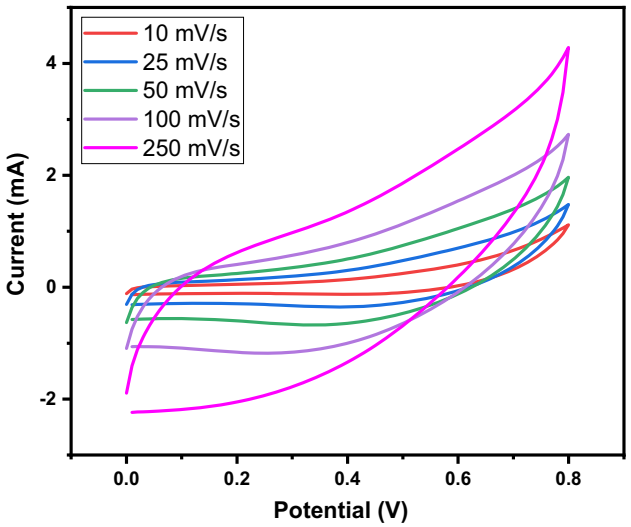

Fig. 8 CV curves of the supercapacitor cell at different scan rates

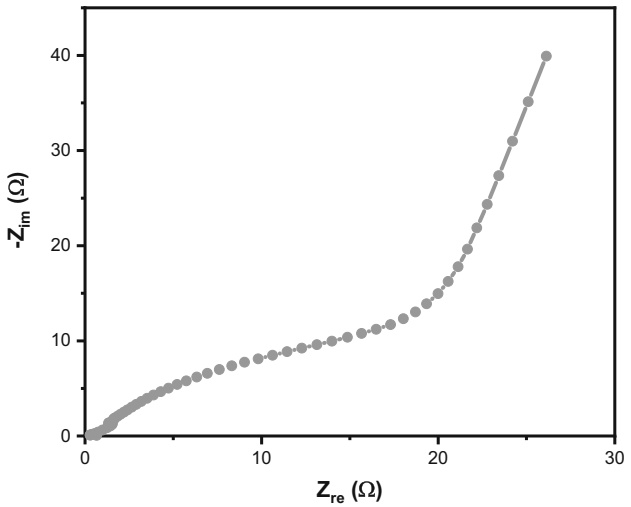

Fig. 9 Impedance graph of the supercapacitor

nafion from TFW-30%Cu catalyst does not show sufficient electrochemical performance. However, a good performance can be obtained by changing the materials and methods used.

4 Conclusions

In the methanolysis and supercapacitor experiments of $NaHB_4$, it was clearly demonstrated in this study that the TFW-30%Cu catalyst, which was synthesized by us for the first time, can be used both in energy storage and in energy production. This bifunctional catalyst was named as "Cap-Cat" [35–38]. Thus, the

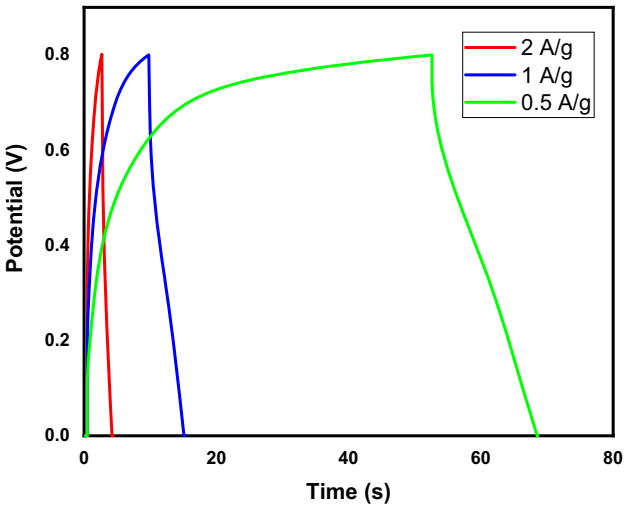

Fig. 10 GCD graph of the supercapacitor at various current intensities

results of the present study can be summarized as follows:

In the presence of four different parameters (metal type, metal amount, carbonization temperature, and carbonization time), methanolysis experiments of $NaBH_4$ were performed and the catalyst with the maximum hydrogen production rate (HPR) was determined. As a result, it was determined that the 30% Cu-doped TFW (TFW-30%Cu) catalyst had a maximum HPR at a carbonization temperature of 300 °C and a carbonization time of 60 min compared to other substances. As a result of the methanolysis experiments performed in the presence of TFW-30%Cu catalyst, the maximum HPR and activation energy were determined as 9475 mL $(min.g)^{-1}$ and 13.02 kJ mol^{-1}, respectively. In supercapacitor application, the capacitance of the electrodes in the presence of TFW-30%Cu was calculated as 7–19.9 $F.(g)^{-1}$.

Acknowledgements

The authors are grateful for the financial support to The Unit of Scientific Research Project Coordination (BAP) at Erciyes University, Kayseri. Project ID: FDK-2020-10493.

Supplementary Information: The online version contains supplementary material available at https://doi.org/10.1007/s10854-021-07275-6.

References

1. R.A. Barreto, Fossil fuels, alternative energy and economic growth. Econ. Model. **75**, 196–220 (2018)
2. T.S. Uyar, D. Beşikci, Integration of hydrogen energy systems into renewable energy systems for better design of 100% renewable energy communities. Int. J. Hydrog. Energy **42**(4), 2453–2456 (2017)
3. B.P. Tarasov, P.V. Fursikov, A.A. Volodin, M.S. Bocharnikov, Y.Y. Shimkus, A.M. Kashin, V.A. Yartys, S. Chidziva, S. Pasupathi, M.V. Lototskyy, Metal hydride hydrogen storage and compression systems for energy storage technologies. Int. J. Hydrog. Energy **46**, 13647 (2020)
4. B.P. Tarasov, M.S. Bocharnikov, Y.B. Yanenko, P.V. Fursikov, K.B. Minko, M.V. Lototskyy, Metal hydride hydrogen compressors for energy storage systems: layout features and results of long-term tests. J. Phys. **2**(2), 024005 (2020)
5. G. Bozkurt, A. Özer, A.B. Yurtcan, Hydrogen generation from sodium borohydride with Ni and Co based catalysts supported on Co3O4. Int. J. Hydrog. Energy **43**(49), 22205–22214 (2018)
6. V. Simagina, A. Ozerova, O. Komova, G. Odegova, D. Kellerman, R. Fursenko, E. Odintsov, O. Netskina, Cobalt boride catalysts for small-scale energy application. Catal. Today **242**, 221–229 (2015)
7. D. Call, B.E. Logan, Hydrogen production in a single chamber microbial electrolysis cell lacking a membrane. Environ. Sci. Technol. **42**(9), 3401–3406 (2008)
8. P.A. Selembo, M.D. Merrill, B.E. Logan, Hydrogen production with nickel powder cathode catalysts in microbial electrolysis cells. Int. J. Hydrog. Energy **35**(2), 428–437 (2010)
9. Y.-X. Huang, X.-W. Liu, X.-F. Sun, G.-P. Sheng, Y.-Y. Zhang, G.-M. Yan, S.-G. Wang, A.-W. Xu, H.-Q. Yu, A new cathodic electrode deposit with palladium nanoparticles for cost-effective hydrogen production in a microbial electrolysis cell. Int. J. Hydrog. Energy **36**(4), 2773–2776 (2011)
10. H. Yuan, J. Li, C. Yuan, Z. He, Facile synthesis of MoS2@CNT as an effective catalyst for hydrogen production in microbial electrolysis cells. ChemElectroChem **1**(11), 1828–1833 (2014)
11. A.K. Avci, Z.I. Önsan, Compr. Energy Syst. **2018**, 475–523 (2018)
12. M. Kaya, M. Bekiroğullari, C. Saka, Highly efficient CoB catalyst using a support material based on Spirulina microalgal strain treated with ZnCl2 for hydrogen generation via sodium borohydride methanolysis. Int. J. Energy Res. **43**(9), 4243–4252 (2019)
13. S.K. Bhattacharya, R.R. Tummala, Next generation integral passives: materials, processes, and integration of resistors and capacitors on PWB substrates. J. Mater. Sci. **11**(3), 253–268 (2000)
14. J. Liang, H. Zhao, L. Yue, G. Fan, T. Li, S. Lu, G. Chen, S. Gao, A.M. Asiri, X. Sun, Recent advances in electrospun nanofibers for supercapacitors. J. Mater. Chem. A **8**(33), 16747–16789 (2020)
15. J. Liu, Y.-G. Xu, L.-B. Kong, Cleverly embedded CoS2/NiS2 on two-dimensional graphene nanosheets as high-performance anode material for improved sodium ion batteries and sodium ion capacitors. J. Mater. Sci. **31**(12), 9946 (2020)
16. S. Vijayalakshmi, E. Elaiyappillai, P.M. Johnson, I.S. Lydia, Multifunctional magnetic CoFe2O4 nanoparticles for the photocatalytic discoloration of aqueous methyl violet dye and energy storage applications. J. Mater. Sci. **31**, 10738–10749 (2020)
17. C. Duran, D. Ozdes, A. Gundogdu, M. Imamoglu, H.B. Senturk, Tea-industry waste activated carbon, as a novel adsorbent, for separation, preconcentration and speciation of chromium. Anal. Chim. Acta **688**(1), 75–83 (2011)
18. C.-H. Weng, Y.-T. Lin, D.-Y. Hong, Y.C. Sharma, S.-C. Chen, K. Tripathi, Effective removal of copper ions from aqueous solution using base treated black tea waste. Ecol. Eng. **67**, 127–133 (2014)
19. A. Gundogdu, C. Duran, H.B. Senturk, M. Soylak, M. Imamoglu, Y. Onal, Physicochemical characteristics of a novel activated carbon produced from tea industry waste. J. Anal. Appl. Pyrolysis **104**, 249–259 (2013)
20. C. Saka, M. Kaya, M. Bekiroğullari, *Chlorella vulgaris* microalgae strain modified with zinc chloride as a new support material for hydrogen production from NaBH4 methanolysis using CuB, NiB, and FeB metal catalysts. Int. J. Hydrog. Energy **45**(3), 1959–1968 (2020)
21. K. Mustafa, M. Bekirogullari, Investigation of hydrogen production from sodium borohydride methanolysis in the presence of Al2O3/spirulina platensis supported Co catalyst. Avrupa Bil. Tekn. Der. **16**, 69–76 (2019)
22. R. Fernandes, N. Patel, A. Miotello, M. Filippi, Studies on catalytic behavior of Co–Ni–B in hydrogen production by hydrolysis of NaBH4. J. Mole. Catal. A **298**(1–2), 1–6 (2009)
23. M. Kaya, NiB loaded acetic acid treated microalgae strain (Spirulina Platensis) to use as a catalyst for hydrogen generation from sodium borohydride methanolysis. Energy Sources Part A **41**(20), 2549–2560 (2019)
24. A. Pinto, D. Falcao, R. Silva, C. Rangel, Hydrogen generation and storage from hydrolysis of sodium borohydride in batch reactors. Int. J. Hydrog. Energy. **31**(10), 1341–1347 (2006)
25. M. Bekirogullari, Catalytic activities of non-noble metal catalysts (CuB, FeB, and NiB) with *C. vulgaris* microalgal strain support modified by using phosphoric acid for

hydrogen generation from sodium borohydride methanolysis. Int. J. Hydrog. Energy **44**(29), 14981–14991 (2019)
26. Y. Wei, W. Meng, Y. Wang, Y. Gao, K. Qi, K. Zhang, Fast hydrogen generation from NABH4 hydrolysis catalyzed by nanostructured CoeNieB catalysts. Int. J. Hydrog. Energy **42**(6072), e6079 (2017)
27. M. Bekiroğullari, M. Kaya, C. Saka, Highly efficient Co-B catalysts with *Chlorella vulgaris* microalgal strain modified using hydrochloric acid as a new support material for hydrogen production from methanolysis of sodium borohydride. Int. J. Hydrog. Energy **44**(14), 7262–7275 (2019)
28. Y. Wei, R. Wang, L. Meng, Y. Wang, G. Li, S. Xin, X. Zhao, K. Zhang, Hydrogen generation from alkaline NaBH4 solution using a dandelion-like Co–Mo–B catalyst supported on carbon cloth. Int. J. Hydrog. Energy **42**(15), 9945–9951 (2017)
29. M. Bekirogullari, Hydrogen production from sodium borohydride by ZnCl2 treated defatted spent coffee ground catalyst. Int. J. Hydrog. Energy. **45**(16), 9733–9743 (2020)
30. E. Fangaj, A.A. Ali, F. Güngör, S. Bektaş, A.A. Ceyhan, The use of metallurgical waste sludge as a catalyst in hydrogen production from sodium borohydride. Int. J. Hydrog. Energy **45**, 13322 (2020)
31. X. Zhu, S. Yu, K. Xu, Y. Zhang, L. Zhang, G. Lou, Y. Wu, E. Zhu, H. Chen, Z. Shen, Sustainable activated carbons from dead ginkgo leaves for supercapacitor electrode active materials. Chem. Eng. Sci. **181**, 36–45 (2018)
32. B. Xu, S. Yue, Z. Sui, X. Zhang, S. Hou, G. Cao, Y. Yang, What is the choice for supercapacitors: graphene or graphene oxide? Energy Environ. Sci. **4**(8), 2826–2830 (2011)
33. F.R.M.S. Raj, N.V. Jaya, G. Boopathi, D. Kalpana, A. Pandurangan, S-doped activated mesoporous carbon derived from the *Borassus flabellifer* flower as active electrodes for supercapacitors. Mater. Chem. Phys. **240**, 122151 (2020)
34. Z. Song, D. Zhu, D. Xue, J. Yan, X. Chai, W. Xiong, Z. Wang, Y. Lv, T. Cao, M. Liu, Nitrogen-enriched hollow porous carbon nanospheres with tailored morphology and microstructure for all-solid-state symmetric supercapacitors. ACS Appl. Energy Mater. **1**(8), 4293–4303 (2018)
35. M. Bolat, C. Yavuz, M. Kaya, Investigation of dual-functionalized novel carbon supported Sn material from corn stalk for energy storage and fuel cell systems on distributed generations. J. Mater. Sci. **2021**, 1–15 (2021)
36. I.I.G. Inal, M. Akdemir, M. Kaya, Microcystis aeruginosa supported-Mn catalyst as a new promising supercapacitor electrode: a dual functional material. Int. J. Hydrog. Energy **46**, 21534 (2021)
37. M. Akdemir, T. Avci Hansu, A. Caglar, M. Kaya, H. Demir Kivrak, Ruthenium modified defatted spent coffee catalysts for supercapacitor and methanolysis application. Energy Storage **3**, e243 (2021)
38. S. Özarslan, M.R. Atelge, M. Kaya, S. Ünalan, Production of dual functional carbon material from biomass treated with NaOH for supercapacitor and catalyst. Energy Storage (2021). https://doi.org/10.1002/est2.257